Earth and Planetary Science Letters 503 (2018) 252–255

Contents lists available at ScienceDirect

Earth and Planetary Science Letters

www.elsevier.com/locate/epsl

Reply to Zhang et al.: Late Miocene–Pliocene magnetochronology of the Shilou Red Clay on the eastern Chinese Loess Plateau

Hong Ao [a,*], Andrew P. Roberts [b], Mark J. Dekkers [c], Xiaodong Liu [a], Eelco J. Rohling [b,d], Zhengguo Shi [a], Zhisheng An [a], Hong Chang [a], Xiaoke Qiang [a], Xiang Zhao [b]

[a] State Key Laboratory of Loess and Quaternary Geology, Institute of Earth Environment, Chinese Academy of Sciences, Xi'an 710061, China
[b] Research School of Earth Sciences, The Australian National University, Canberra 2601, Australia
[c] Paleomagnetic Laboratory 'Fort Hoofddijk', Department of Earth Sciences, Faculty of Geosciences, Utrecht University, Budapestlaan 17, 3584 CD Utrecht, the Netherlands
[d] Ocean and Earth Science, University of Southampton, National Oceanography Centre, Southampton SO14 3ZH, UK

ARTICLE INFO

Article history:
Received 6 August 2018
Accepted 16 August 2018
Editor: B. Buffett

We thank Zhang et al. (2018) for their comments on our paper (Ao et al., 2016). Here we take the opportunity to clarify our approach in support of its robustness.

The Chinese Loess Plateau (CLP) hosts a vast expanse (∼300,000 km^2) of thick eolian dust deposits that consist of the well-known Quaternary loess–paleosol sequence and the underlying Miocene–Pliocene Red Clay sequence (Fig. 1). The Shilou Red Clay section is a typical eolian Red Clay section on the eastern CLP. Xu et al. (2009) reported that the ∼70-m thick Shilou Red Clay (here named the Shilou-A section) spanned from polarity subchron C5n.2n to C2An.1n, with an age of ∼11–2.6 Ma, while Anwar et al. (2015) revised its age to ∼5.2–2.6 Ma (from C3n.4n to C2An.1n). Recently, we reported an updated magnetostratigraphy from a new Shilou Red Clay section with a thickness of ∼90-m (here named the Shilou-B section), which is situated ∼1 km from the Shilou-A section (Ao et al., 2016). Our updated magnetostratigraphy from the 90-m thick Shilou-B section, which has a much higher sampling resolution and significantly improved polarity zone definition compared to previous studies, enables unequivocal magnetostratigraphic correlation (C4r.1r–C2An.1n, ∼8.2–2.6 Ma) to the geomagnetic polarity time scale (GPTS) of Hilgen et al. (2012) (Fig. 2). This results in a reassigned correlation of the ∼70-m thick Shilou-A magnetostratigraphy to the GPTS from C4n.2n to C2An.1n, with an age of ∼8–2.6 Ma. The main point of Zhang et al. (2018) is that the Shilou Red Clay could have a Pliocene (Anwar et al., 2015) rather than Late Miocene–Pliocene age (Xu et al., 2009; Ao et al., 2016), and that a cyclostratigraphic approach is essential when developing age models based mainly on magnetostratigraphic results without additional age constraints. Here we provide chronological evidence in support of our age model for the Shilou Red Clay (Ao et al., 2016, 2018).

Our age assignment for the Shilou Red Clay is consistent with results from other Red Clay sequences on the central and eastern CLP, such as the Lingtai (Sun et al., 1998a), Xifeng (Sun et al., 1998b), Chaona (Song et al., 2001), and Jiaxian (Qiang et al., 2001) sections, which range in age from 8–7 Ma to 2.6 Ma. Our new magnetostratigraphy, together with these well-established magnetostratigraphic records, suggests that Red Clay sections from across the CLP have consistent magnetostratigraphic sequences, although sedimentation rates, lithology, and stratigraphic continuity vary (Fig. 2). For the uppermost Red Clay, a distinctive pattern of three normal polarity intervals (N1, N2, and N3) separated by two short reversed polarity intervals (R2 and R3) enables unequivocal correlation to chrons C2An.1n to C2An.3n across the CLP. The underlying four normal polarity intervals (N4, N5, N6, and N7), which are separated by three reversed polarity intervals (R5, R6, and R7), span from chrons C3n.1n to C3n.4n. Two normal polarity intervals (N8 and N9) separated by a reversed polarity interval (R9) in the middle of the successions correlate to chrons C3An.1n and C3An.2n. Normal polarity intervals N10, N13, and N14 in the lower part of the successions are correlated to C3Bn, C4n.1n, and C4n.2n, respectively. This magnetostratigraphic assignment matches consistently with the structure of the Late Miocene–Pliocene GPTS (Fig. 2).

DOI of original article: https://doi.org/10.1016/j.epsl.2016.03.028.
DOI of comment: https://doi.org/10.1016/j.epsl.2018.08.033.
* Corresponding author. Address: No. 97 Yanxiang Road, Xi'an 710061, Shaanxi, China.
E-mail address: aohong@ieecas.cn (H. Ao).

https://doi.org/10.1016/j.epsl.2018.08.045
0012-821X/

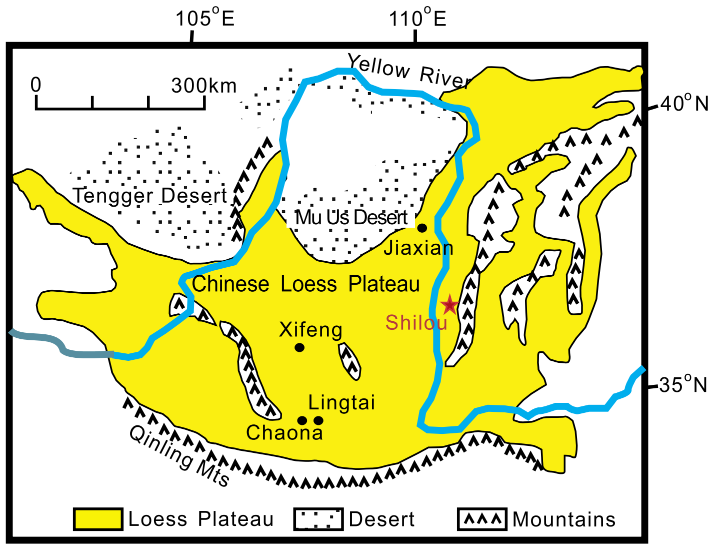

Fig. 1. Map of the Chinese Loess Plateau with locations of the studied Shilou and other Red Clay sections mentioned in the text.

Our updated age model for the Shilou Red Clay is also supported by magnetic susceptibility (χ) variations of the Red Clay across the CLP. For example, two typical χ peaks (A and B) in the uppermost Red Clay are located within normal polarity chron C2An.1n at all of the Shilou, Jiaxian, Chaona, Xifeng, and Lingtai sections. The underlying χ peaks C, D, and E are located consistently around C2An.2n, C2An.3n, and in lower C2Ar to upper C3n.1n, respectively. χ peaks F and G in the middle Red Clay successions are consistently located around C3n.4n and lower C3r to upper C3An.1n, respectively. This suggests that the upper Red Clay successions span at least from C2An.1n to C3An.1n and are older than 6 Ma. Therefore, correlation of the polarity record to the GPTS in the lower Red Clay successions is unlikely to have a Pliocene age as argued by Zhang et al. (2018) and Anwar et al. (2015).

Zhang et al. (2018) argue that the finding of a tooth of *Meriones sp*. at 46.6 m in the Shilou-A section by Xu et al. (2012) cannot be used as an independent Late Miocene biochronological constraint on the magnetostratigraphic interpretation. This appears to be a misunderstanding that we seek to clarify here. The Late Miocene age for *Meriones sp*. is not based on the magnetostratigraphy of Xu et al. (2009), but is inferred independently from its biochronology across the CLP (Zheng and Zhang, 2000, 2001). *Meriones sp*. is an important small mammal that lived across the CLP in the Late Miocene (Zheng and Zhang, 2000, 2001; Xu et al., 2012). Thus, its presence in the Shilou-A section provides useful independent support for our chronology. Furthermore, our updated high-resolution magnetostratigraphy is supported by the paleomagnetic and χ correlation among other Red Clay successions (e.g. Lingtai) that are constrained precisely by biochronology (Zheng and Zhang, 2000, 2001).

In contrast to our chronology for the Shilou Red Clay, Anwar et al. (2015) and Zhang et al. (2018) argue that (Fig. 2, right-hand side): (1) the uppermost three normal polarity intervals (N1, N2, and N3) and two intercalated reversed polarity intervals (R2 and R3) correlate to normal polarity chron C2An.1n; (2) the underlying two normal polarity intervals N4 and N5 separated by a reversed polarity interval R5 correlate to normal polarity chron C2An.2n; (3) normal polarity intervals N6 and N7 separated by reversed polarity interval R7 correlate to normal polarity chron C2An.3n; (4) normal polarity intervals N8 and N9 correlate to normal polarity chrons C3n.1n and C3n.2n; (5) normal polarity intervals N10 and N11 separated by reversed polarity interval R11 correlate to normal polarity chron C3n.2n; and (6) normal polarity intervals N14 and N15 separated by reversed polarity interval R15 correlate to normal polarity chron C3n.4n. This, in our view, incorrect magnetostratigraphic correlation would lead to an age of ∼5.2–2.6 Ma for the Shilou Red Clay. First, this magnetostratigraphic correlation is inconsistent with the established paleomagnetic and χ chronology of the Red Clay across the CLP (Fig. 2) and would require complete reinterpretation of the Red Clay chronology. For example, our data and the existing body of data from other Red Clay sections suggest that the marked boundary between the Baode and Jingle Formations, which occurs at the initiation of χ peak F, is located close to the Miocene–Pliocene boundary. The Pliocene Jingle Formation has a distinctly redder colour than the Late Miocene Baode Formation, which is consistent with enhanced pedogenesis and increased summer monsoon precipitation across the Miocene–Pliocene boundary (Zhu et al., 2008; Ao et al., 2018). In contrast, according to the magnetostratigraphic correlation of Zhang et al. (2018) and Anwar et al. (2015), the boundary between the Baode and Jingle Formations would be placed erroneously within the middle Pliocene at ∼3.6 Ma.

The magnetostratigraphic correlation of Anwar et al. (2015) and Zhang et al. (2018) is also inconsistent with the structure of the GPTS. Based on the argument that polarity zones with durations <30 kyr relate to geomagnetic excursions, they ignore several normal and particularly reversed polarity zones while other polarity zones with similar thicknesses are retained in their polarity zonation. A 30-kyr duration is equivalent to a ∼0.5 m thickness in the Ao et al. (2016) age model and to a ∼0.8 m thickness in the Anwar et al. (2015) age model. Polarity features with <30 kyr duration are referred to by Cande and Kent (1992) as cryptochrons. The nature of cryptochrons has been much debated. Cryptochrons could represent polarity intervals with durations <30 kyr, which are too short to be well defined in marine magnetic anomaly records, and that, therefore, are not included in the GPTS. Zhang et al. (2018) suggest that polarity features with durations <30 kyr are equivalent to geomagnetic excursions. There is no consensus to support this interpretation. Excursion durations are not well constrained, but the most precise estimates for field intensity minima associated with excursions, based on cosmogenic isotope records in ice cores with chronologies based on annual layer counting, are in the 1–3 kyr range (Roberts, 2008). Directional excursions tend to be shorter than the accompanying paleointensity minima. It is, therefore, unlikely that relatively thick polarity intervals in the Red Clay represent geomagnetic excursions as argued by Zhang et al. (2018). We acknowledge that alternative interpretations are possible with some of the thinner polarity zones identified in Red

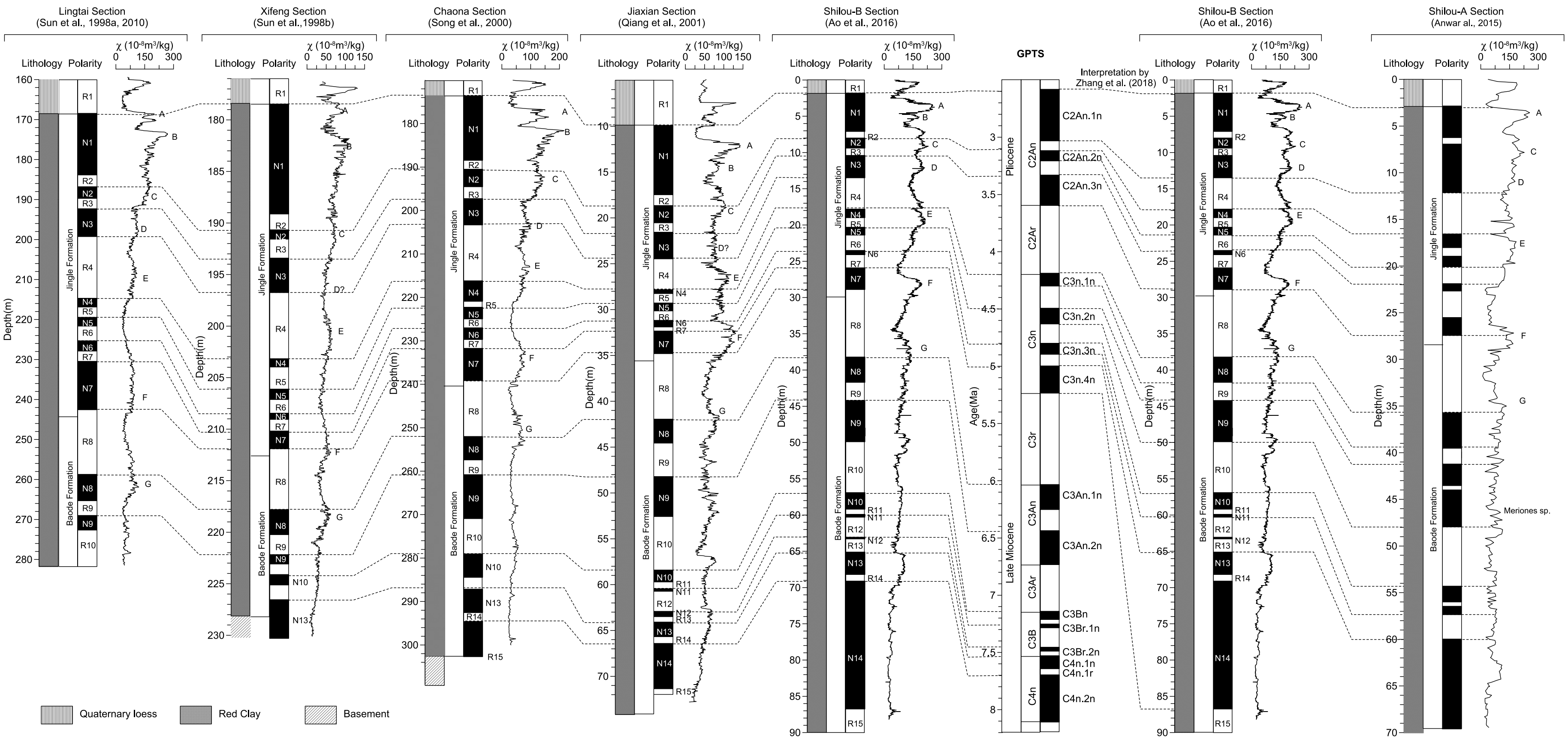

Fig. 2. Comparison of the lithostratigraphy, χ, and paleomagnetic polarity stratigraphy of the Shilou Red Clay from Ao et al. (2016) and Zhang et al. (2018). Lithostratigraphy and magnetostratigraphy for Red Clay sections from Lingtai (Sun et al., 1998a, 2010), Xifeng (Sun et al., 1998b), Chaona (Song et al., 2001), and Jiaxian (Qiang et al., 2001) across the CLP, and their correlation to the GPTS (Hilgen et al., 2012). In contrast to our high-resolution magnetostratigraphy and lithostratigraphy of the Shilou Red Clay (Ao et al., 2016) that is highly consistent with that of other Red Clay successions and GPTS, the magnetostratigraphic correlation of Zhang et al. (2018) and Anwar et al. (2015) has a less consistent correlation with the structure of GPTS and that of other Red Clay successions.

Clay representing short polarity intervals that are not recognized in the GPTS. However, there is significant arbitrariness in making these definitions in the chronology proposed by Anwar et al. (2015) and Zhang et al. (2018). Zhang et al. (2018) comment that "Events" (2), (4), and (5) are significantly thicker than 1 m, so why do they ignore them? The reversed polarity zone (R6) between "Events" (4) and (5) has a similar thickness as those "Events", so why is it not ignored? A notably thick reversed polarity zone in the Shilou-A section (∼4 m, at the ∼22.7–26.5 m stratigraphic level, Anwar et al., 2015) is also put aside and is correlated with the two straddling normal polarity zones to C2An.3n. With the 2.6 cm/kyr accumulation rate in the age model of Anwar et al. (2015), this interval would have a ∼160 kyr duration, which should be detected in the GPTS (Hilgen et al., 2012). The thinner reversed polarity interval (∼20–22 m) above it (Shilou-A section) is retained and the next higher reversed polarity zone (∼18–19 m) with approximately equal thickness is also ignored. This arbitrariness is unconvincing, and is not consistent with the standard practice of ensuring that a polarity interpretation matches the polarity pattern in the GPTS. "Events" (6) and (7) of Zhang et al. (2018) correspond to short polarity chrons C3Br.1n and C3Br.2n in the Ao et al. (2016) correlation; polarity chrons C3Br.1n and C3Br.2n have 34 and 35 kyr durations, respectively, in the GPTS (Hilgen et al., 2012). "Event" (8) is correlated by Ao et al. (2016) to a polarity chron (C4n.1r) with 114 kyr duration (Hilgen et al., 2012).

In the age model of Anwar et al. (2015) and Zhang et al. (2018), polarity zones indicated as "Events" would be geomagnetic excursions, with two reversed polarity excursions in chron C2An.1n, one in C2An.2n, one in C2An.3n, one in C3n.3n, and one in C3n.4n. Eolian Red Clay has a low sedimentation rate of 1–2 cm/kyr and, therefore, is unlikely to record potential geomagnetic excursions (e.g., Roberts, 2008). The overlying Quaternary loess has higher accumulation rates, but only the most rapidly deposited units contain thin excursion records (Pan et al., 2002; Liu et al., 2015). Established magnetostratigraphic records from across the CLP have not yet documented the presence of geomagnetic excursions in the Red Clay. Zhang et al. (2018) invoke arguments that would require the Shilou sequence to have a chronology that is inconsistent with the generally accepted age from ∼8–7 Ma to 2.6 Ma for Red Clay successions on the CLP (e.g., Lingtai, Xifeng, Chaona, and Jiaxian) and would require what is in our view an erroneous age of ∼5.2–2.6 Ma. Our updated high-resolution paleomagnetic and χ chronology for the Shilou-B section of ∼8–2.6 Ma is consistent with that of other Red Clay successions, and particularly with the GPTS chron structure.

We agree with Zhang et al. (2018) that cyclostratigraphy is a useful tool for age model refinement. However, a cyclostratigraphy must be developed as part of an integrated stratigraphic approach. Without age constraints from robust magnetostratigraphy or other numerical dating, fundamental mistakes can still be made in an age model established by a combination of an erroneous magnetostratigraphy and cyclostratigraphy. Erroneous age constraints from incorrect magnetostratigraphic correlations ensure that the use of cyclostratigraphy by Anwar et al. (2015) neither results in a correct age model nor reveals the correct Milankovitch cycles in the Shilou Red Clay, and leads to erroneous paleoclimatic interpretations. The final "optimally tuned" age model proposed by Anwar et al. (2015), unfortunately, does not express cyclicity straightforwardly.

Acknowledgements

This study was financially supported by the Key Research Program of Frontier Sciences, Chinese Academy of Sciences (grants QYZDB-SSW-DQC021, QYZDY-SSW-DQC001, and ZDBS-SSW-DQC001).

References

Anwar, T., Kravchinsky, V.A., Zhang, R., 2015. Magneto- and cyclostratigraphy in the red clay sequence: new age model and paleoclimatic implication for the eastern Chinese Loess Plateau. J. Geophys. Res. 120, 6758–6770.

Ao, H., Dekkers, M.J., Roberts, A.P., Rohling, E.J., An, Z.S., Liu, X.D., Jiang, Z.X., Qiang, X.K., Xu, Y., Chang, H., 2018. Mineral magnetic record of the Miocene–Pliocene climate transition on the Chinese Loess Plateau, North China. Quat. Res. 89, 619–628.

Ao, H., Roberts, A.P., Dekkers, M.J., Liu, X.D., Rohling, E.J., Shi, Z.G., An, Z.S., 2016. Late Miocene–Pliocene Asian monsoon intensification linked to Antarctic ice-sheet growth. Earth Planet. Sci. Lett. 444, 75–87.

Cande, S.C., Kent, D.V., 1992. A new geomagnetic polarity time scale for the Late Cretaceous and Cenozoic. J. Geophys. Res. 97, 13917–13951.

Hilgen, F.J., Lourens, L.J., van Dam, J.A., 2012. The Neogene period. In: Gradstein, F.M., Ogg, J.G., Schmitz, M., Ogg, G. (Eds.), The Geologic Time Scale 2012. Elsevier, Amsterdam, pp. 923–978.

Liu, Q.S., Jin, C.S., Hu, P.X., Jiang, Z.X., Ge, K.P., Roberts, A.P., 2015. Magnetostratigraphy of Chinese loess–paleosol sequences. Earth-Sci. Rev. 150, 139–167.

Pan, Y.X., Zhu, R.X., Liu, Q.S., Guo, B., Yue, L.P., Wu, H.N., 2002. Geomagnetic episodes of the last 1.2 Myr recorded in Chinese loess. Geophys. Res. Lett. 29, 1282. https://doi.org/10.1029/2001GL014024.

Qiang, X.K., Li, Z.X., Powell, C.M., Zheng, H.B., 2001. Magnetostratigraphic record of the Late Miocene onset of the East Asian monsoon, and Pliocene uplift of northern Tibet. Earth Planet. Sci. Lett. 187, 83–93.

Roberts, A.P., 2008. Geomagnetic excursions: knowns and unknowns. Geophys. Res. Lett. 35, L17307. https://doi.org/10.11029/12008GL034719.

Song, Y.G., Fang, X.M., Torii, M., Naoto, I., Li, J.J., An, Z.S., 2001. Magnetostratigraphy of Late Tertiary sediments from the Chinese Loess Plateau and its paleoclimatic significance. Chin. Sci. Bull. 46, 16–22.

Sun, D.H., Shaw, J., An, Z.S., Cheng, M.Y., Yue, L.P., 1998a. Magnetostratigraphy and paleoclimatic interpretation of a continuous 7.2 Ma Late Cenozoic eolian sediments from the Chinese Loess Plateau. Geophys. Res. Lett. 25, 85–88.

Sun, D.H., An, Z.S., Shaw, J., Bloemendal, J., Sun, Y.B., 1998b. Magnetostratigraphy and palaeoclimatic significance of late Tertiary aeolian sequences in the Chinese Loess Plateau. Geophys. J. Int. 134, 207–212.

Sun, Y.B., An, Z.S., Clemens, S.C., Bloemendal, J., Vandenberghe, J., 2010. Seven million years of wind and precipitation variability on the Chinese Loess Plateau. Earth Planet. Sci. Lett. 297, 525–535.

Xu, Y., Yue, L.P., Li, J.X., Sun, L., Sun, B., Zhang, J.Y., Ma, J., Wang, J.Q., 2009. An 11-Ma-old red clay sequence on the Eastern Chinese Loess Plateau. Palaeogeogr. Palaeoclimatol. Palaeoecol. 284, 383–391.

Xu, Y., Yue, L.P., Li, J.X., Sun, L., Sun, B., Zhang, J.Y., Ma, J., Wang, J.Q., 2012. Red clay deposits on the Chinese Loess Plateau during 11.0–2.6 Ma and its implications for long-term evolution of East Asian monsoon. Environ. Earth Sci. 66, 2021–2030.

Zhang, R., Kravchinsky, V.A., Anwar, T., Yue, L.P., Li, J.X., Jiao, J., 2018. Comment on "Late Miocene–Pliocene Asian monsoon intensification linked to Antarctic ice-sheet growth". Earth Planet. Sci. Lett. 503, 248–251 (this issue).

Zheng, S.H., Zhang, Z.Q., 2000. Late Miocene–early Pleistocene micromammals from Wenwanggou of Lingtai, Gansu, China. Vertebrata PalAsiatica 38, 58–71.

Zheng, S.H., Zhang, Z.Q., 2001. Late Miocene–early Pleistocene biostratigraphy of the Leijiahe area, Lingtai, Gansu. Vertebrata PalAsiatica 39, 215–228.

Zhu, Y.M., Zhou, L.P., Mo, D.W., Kaakinen, A., Zhang, Z.Q., Fortelius, M., 2008. A new magnetostratigraphic framework for late Neogene Hipparion Red Clay in the eastern Loess Plateau of China. Palaeogeogr. Palaeoclimatol. Palaeoecol. 268, 47–57.